

# Phase diagram of the D3/D5 system in a magnetic field and a BKT transition

Nick Evans,<sup>\*</sup> Astrid Gebauer,<sup>†</sup> Keun-Young Kim,<sup>‡</sup> and Maria Magou<sup>§</sup>  
*School of Physics and Astronomy,  
University of Southampton,  
Southampton, SO17 1BJ, UK*

We study the full temperature and chemical potential dependence of the D3/D5 2+1 dimensional theory in the presence of a magnetic field. The theory displays separate transitions associated with chiral symmetry breaking and melting of the bound states. We display the phase diagram which has areas with first and second order transitions meeting at two critical points similar to that of the D3/D7 system. In addition there is the recently reported BKT transition at zero temperature leading to distinct structure at low temperatures.

## I. INTRODUCTION

There has been recent interest in holographic descriptions of the phase structure of gauge theories in the presence of magnetic fields [1–8]. The D3/D7 holographic system describes a confining 3+1d gauge theory with quarks [9]. The magnetic field induces chiral symmetry breaking. The symmetry breaking and quark confinement are lost at high temperature and density. Between is a rich structure of phase transitions of both first and second order meeting at critical points. These transitions have been explored in [4] and the summary phase diagram is displayed in Fig 1a. Here the theory is interesting as a loose analogue for QCD which is also a confining and chiral symmetry breaking gauge theory but where we can not as yet compute the precise phase diagram.

Interest has also turned to the D3/D5 system [10] that describes fundamental representation matter fields on a 2+1d defect within a 3+1d gauge theory. This system may have some lessons for condensed matter systems. In [7] an analysis of the D3/D5 system at finite density ( $d$ ) and at zero temperature ( $T$ ) revealed that the chiral symmetry breaking transition with increasing magnetic field ( $B$ ) is not second order but similar to a Berezinskii-Kosterlitz-Thouless (BKT) transition [11] (see also the holographic example in [8, 12]). That is order parameters across the transition grow as  $\exp(-a/\sqrt{\nu_c - \nu})$  where  $a$  is a constant and  $\nu = d/B$ . ( $\nu_c$  the critical value for the transition). For small  $T$  the authors of [7] showed the BKT transition returns to a second order nature. This difference from the D3/D7 case is surprising so it seems worth fleshing out the entire phase diagram for the theory to see if other surprises are present. In this letter we present that analysis - much of the computation matches that in the D3/D7 system which we worked through in detail in [4] so here we very briefly present the formalism and the conclusions. We display the resulting phase dia-

gram for massless matter fields in Fig 1b. Clearly much of the structure is similar to the D3/D7 case but the second order boundary of the chiral symmetry breaking phase is distorted by the presence of the BKT transition.

## II. THE HOLOGRAPHIC DESCRIPTION

The  $\mathcal{N}=4$  super Yang-Mills gauge theory at finite temperature has a holographic description in terms of an  $\text{AdS}_5$  black hole geometry (with  $N$  D3 branes at its core)[13]. The geometry can be written as

$$ds^2 = \frac{w^2}{R^2}(-g_t dt^2 + g_x d\vec{x}^2 + g_y dy^2) + \frac{R^2}{w^2}(d\rho^2 + \rho^2 d\Omega_2^2 + dL^2 + L^2 d\bar{\Omega}_2^2), \quad (1)$$

where  $\vec{x}$  is two dimensional,  $y$  will be the D3 coordinate not shared by our D5, we have split the transverse six plane into two three planes each with a radial coordinate  $\rho, L$  and a two sphere,  $R^4 = 4\pi g_s N \alpha'^2$  and

$$g_t := \frac{(w^4 - w_H^4)^2}{2w^4(w^4 + w_H^4)}, \quad g_x := \frac{w^4 + w_H^4}{2w^4}. \quad (2)$$

The temperature of the theory is given by the position of the horizon,  $w_H = \pi R^2 T$

We include our 2+1d defect with fundamental matter fields by placing a probe D5 brane in the D3 geometry. The probe limit corresponds to the quenched limit of the gauge theory. The D5 probe can be described by its DBI action

$$S_{DBI} = -T_{D5} \int d^6 \xi \sqrt{-\det(P[G]_{ab} + 2\pi\alpha' F_{ab})}, \quad (3)$$

where  $P[G]_{ab}$  is the pullback of the metric and  $F_{ab}$  is the gauge field living on the D5 world volume. We will use  $F_{ab}$  to introduce a constant magnetic field (eg  $F_{12} = -F_{21} = B$ ) [1] and a chemical potential associated with baryon number  $A_t(\rho) \neq 0$  [14, 15] We embed the D5 brane in the  $t, \vec{x}, \rho$  and  $\Omega_2$  directions of the metric but to allow all possible embeddings must include a profile  $L(\rho)$

<sup>\*</sup>Electronic address: evans@soton.ac.uk

<sup>†</sup>Electronic address: ag806@soton.ac.uk

<sup>‡</sup>Electronic address: k.kim@soton.ac.uk

<sup>§</sup>Electronic address: mm21g08@soton.ac.uk

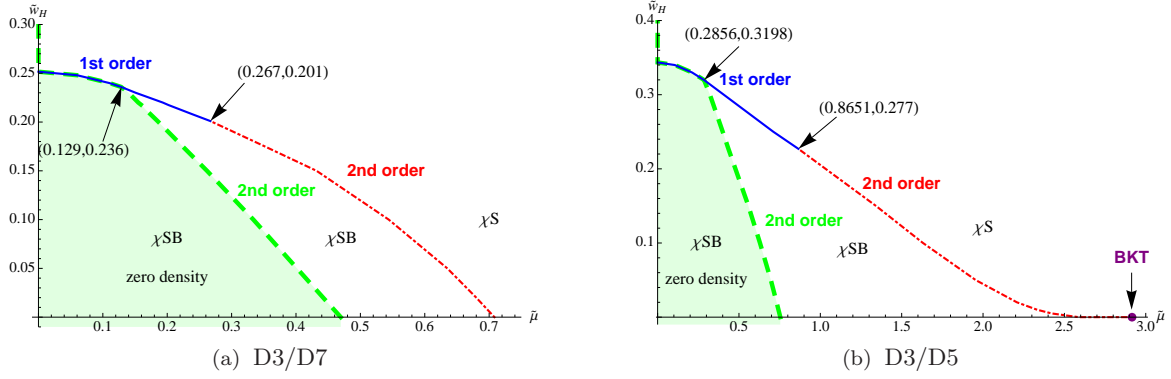


FIG. 1: The phase diagrams for the D3/D7 [4] and D3/D5 systems.  $\tilde{w}_H$  measure the temperature of the theory whilst  $\tilde{\mu}$  is the chemical potential. The dashed line is a second order transition associated with the formation of quark density and meson melting. The dotted line is a second order transition for chiral symmetry restoration. In the D3/D5 case that transition ends at a BKT transition point and its effects on the second order line can be seen. The continuous line is the merged first order transition. The position of critical points are marked.

at constant  $y, \bar{\Omega}_2$ . The full DBI action we will consider is then

$$S = \int d\xi^6 \mathcal{L}(\rho) = \left( \int_{S^2} \epsilon_2 \int dt d\vec{x} \right) \int d\rho \mathcal{L}(\rho), \quad (4)$$

where  $\epsilon_2$  is a volume element on the 2-sphere and

$$\begin{aligned} \mathcal{L} := & -N_f T_{D5} \frac{\rho^2}{2\sqrt{2}} \left( 1 - \frac{w_H^4}{w^4} \right) \\ & \times \sqrt{\left( 1 + (\partial_\rho L)^2 - \frac{2w^4(w^4 + w_H^4)}{(w^4 - w_H^4)^2} (2\pi\alpha' \partial_\rho A_t)^2 \right)} \\ & \times \sqrt{\left( \left( 1 + \frac{w_H^4}{w^4} \right) + \frac{4R^4}{w^4 + w_H^4} B^2 \right)}. \end{aligned} \quad (5)$$

Since the action is independent of  $A_t$ , there is a conserved quantity  $d$  ( $:= \frac{\delta S}{\delta F_{\rho t}}$ ) and we can use the Legendre transformed action

$$\tilde{S} = S - \int d\xi^6 F_{\rho t} \frac{\delta S}{\delta F_{\rho t}} = \left( \int_{S^2} \epsilon_2 \int dt d\vec{x} \right) \int d\rho \tilde{\mathcal{L}}(\rho), \quad (6)$$

where

$$\tilde{\mathcal{L}} := -N_f T_{D5} \frac{(w^4 - w_H^4)}{2\sqrt{2}w^4} \sqrt{K(1 + (\partial_\rho L)^2)} \quad (7)$$

$$\begin{aligned} K := & \left( \frac{w^4 + w_H^4}{w^4} \right) \rho^4 + \frac{4R^4 B^2}{w^4 + w_H^4} \rho^4 \\ & + \frac{4w^4}{(w^4 + w_H^4)} \frac{d^2}{(N_f T_{D5} 2\pi\alpha')^2}. \end{aligned} \quad (8)$$

To simplify the analysis we note that we can use the magnetic field value as the intrinsic scale of conformal symmetry breaking in the theory - that is we can rescale

all quantities in (7) by  $B$  to give

$$\tilde{\mathcal{L}} = -N_f T_{D3} (R\sqrt{B})^3 \frac{\tilde{w}^4 - \tilde{w}_H^4}{\tilde{w}^4} \sqrt{\tilde{K}(1 + \tilde{L}^2)}, \quad (9)$$

$$\tilde{K} = \left( \frac{\tilde{w}^4 + \tilde{w}_H^4}{\tilde{w}^4} \right) \tilde{\rho}^4 + \frac{1}{\tilde{w}^4 + \tilde{w}_H^4} \tilde{\rho}^4 + \frac{\tilde{w}^4}{(\tilde{w}^4 + \tilde{w}_H^4)} \tilde{d}^2 \quad (10)$$

where the dimensionless variables are defined as

$$\begin{aligned} (\tilde{w}, \tilde{L}, \tilde{\rho}, \tilde{d}) & \quad (11) \\ := & \left( \frac{w}{R\sqrt{2B}}, \frac{L}{R\sqrt{2B}}, \frac{\rho}{R\sqrt{2B}}, \frac{d}{(R\sqrt{B})^2 N_f T_{D5} 2\pi\alpha'} \right). \end{aligned}$$

In all cases the embeddings become flat at large  $\rho$  taking the form

$$\tilde{L}(\tilde{\rho}) \sim \tilde{m} + \frac{\tilde{c}}{\tilde{\rho}}, \quad (12)$$

In the absence of temperature, magnetic field and density the regular embeddings are simply  $L(\tilde{\rho}) = \tilde{m}$ , which is the minimum length of a D3-D5 string, allowing us to identify it with the quark mass as shown.  $\tilde{c}$  should then be identified with the quark condensate.

We will classify the D5 brane embeddings by their small  $\tilde{\rho}$  behavior. If the D5 brane touches the black hole horizon, we call it a black hole embedding, otherwise, we call it a Minkowski embedding. We have used Mathematica to solve the equations of motion for the D5 embeddings resulting from (9). Typically in what follows, we numerically shoot out from the black hole horizon (for black hole embeddings) or the  $\tilde{\rho} = 0$  axis (for Minkowski embeddings) with Neumann boundary condition for a given  $\tilde{d}$ . Then by fitting the embedding function with (12) at large  $\tilde{\rho}$  we can read off  $\tilde{m}$  and  $\tilde{c}$ .

The Hamilton's equations from (6) are  $\partial_\rho d = \frac{\delta \tilde{S}}{\delta A_t}$  and  $\partial_\rho A_t = -\frac{\delta \tilde{S}}{\delta d}$ . The first simply means that  $d$  is the con-

served quantity. The second reads as

$$\partial_{\tilde{\rho}} \tilde{A}_t = \tilde{d} \frac{\tilde{w}^4 - \tilde{w}_H^4}{\tilde{w}^4 + \tilde{w}_H^4} \sqrt{\frac{1 + (\tilde{L}')^2}{\tilde{K}}}, \quad (13)$$

where  $\tilde{A}_t := \frac{\sqrt{2} 2\pi \alpha' A_t}{R\sqrt{2B}}$ .

There is a trivial solution of (13) with  $\tilde{d} = 0$  and constant  $\tilde{A}_t$  [16]. The embeddings are then the same as those at zero chemical potential. For a finite  $\tilde{d}$ ,  $\tilde{A}_t$  is singular at  $\tilde{\rho} = 0$  and requires a source. In other words the electric displacement must end on a charge source. The source is the end point of strings stretching between the D5 brane and the black hole horizon. The string tension pulls the D5 branes to the horizon resulting in black hole embeddings [14]. For such an embedding the chemical potential ( $\tilde{\mu}$ ) is defined as

$$\begin{aligned} \tilde{\mu} &:= \lim_{\tilde{\rho} \rightarrow \infty} \tilde{A}_t(\tilde{\rho}) \\ &= \int_{\tilde{\rho}_H}^{\infty} d\tilde{\rho} \tilde{d} \frac{\tilde{w}^4 - \tilde{w}_H^4}{\tilde{w}^4 + \tilde{w}_H^4} \frac{\sqrt{1 + (\tilde{L}')^2}}{\sqrt{\tilde{K}}}, \end{aligned} \quad (14)$$

where we fixed  $\tilde{A}_t(\tilde{\rho}_H) = 0$  for a well defined  $A_t$  at the black hole horizon.

The generic analysis below with massless quarks and  $B$ ,  $T$  and  $\mu$  all switched on involve four types of solution of the Euler Lagrange equations. All of these approach the  $\tilde{\rho}$  axis at large  $\rho$  to give a zero quark mass. Firstly, there are Minkowski embeddings that avoid the black hole so have a non-zero condensate  $\tilde{c}$  - these solutions have  $\tilde{d} = 0$  so  $\tilde{A}_t = \mu$ . Secondly, there can be generic black hole solutions with both of  $\tilde{c}$  and  $\tilde{d}$  none zero. Finally there are solutions that lie entirely along the  $\tilde{\rho}$  axis so that  $\tilde{c} = 0$  but with  $\tilde{d}$  either zero or non zero. In fact the flat embeddings with  $\tilde{d} = 0$  are always the energetically least preferred but the other three all play a part in the phase diagram of the theory.

To compare these solutions we compute the relevant thermodynamic potentials. The Euclideanized on shell bulk action can be interpreted as the thermodynamic potential of the boundary field theory. The Grand potential ( $\tilde{\Omega}$ ) is associated with the action (5) while the Helmholtz free energy ( $\tilde{F}$ ) is associated with the Legendre transformed action (6):

$$\begin{aligned} \tilde{F}(\tilde{w}_H, \tilde{d}) &:= \frac{-\tilde{S}}{N_f T_{D5} (R\sqrt{B})^3 \text{Vol}} \\ &= \int_{\tilde{\rho}_H}^{\infty} d\tilde{\rho} \frac{\tilde{w}^4 - \tilde{w}_H^4}{\tilde{w}^4} \sqrt{(1 + (\tilde{L}')^2)} \sqrt{\tilde{K}} \end{aligned} \quad (15)$$

$$\begin{aligned} \tilde{\Omega}(\tilde{w}_H, \tilde{\mu}) &:= \frac{-S}{N_f T_{D5} (R\sqrt{B})^3 \text{Vol}} \\ &= \int_{\tilde{\rho}_H}^{\infty} d\tilde{\rho} \frac{\tilde{w}^4 - \tilde{w}_H^4}{\tilde{w}^4} \sqrt{(1 + (\tilde{L}')^2)} \frac{\tilde{K}(\tilde{d} = 0)}{\sqrt{\tilde{K}}} \end{aligned} \quad (16)$$

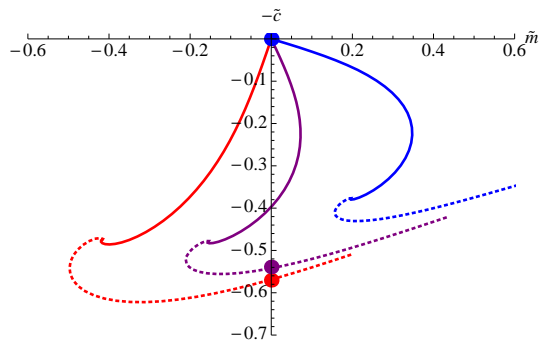


FIG. 2: A plot of the condensate vs the quark mass to show the first order phase transition at zero chemical potential induced by temperature. The solid line corresponds to the black hole embedding and the dotted line to a Minkowski embedding. From bottom to top the curves correspond to temperatures  $\tilde{w}_H = 0.25, 0.3435, 0.45$ .

where Vol denote the trivial 5-dimensional volume integral except  $\tilde{\rho}$  space, so the thermodynamic potentials defined above are densities, strictly speaking. Since  $\tilde{K} \sim \tilde{\rho}^4$ , both integrals diverge as  $\tilde{\rho}^2$  at infinity and need to be renormalized.

### III. CHIRAL SYMMETRY RESTORATION BY TEMPERATURE

The chiral symmetry restoration transition by temperature is first order [6] (a transition related to the thermal transition for non-zero mass at  $B=0$  [17]). The transition on the gravity side is between a Minkowski embedding that avoids the black hole to an embedding that lies along the  $\tilde{\rho}$  axis ending on the black hole. Fig 2 shows the  $(-\tilde{c}, \tilde{m})$  diagram for some temperatures ( $\tilde{w}_H = 0.25, 0.3435, 0.45$  from the bottom). The solid lines are the black hole embeddings and the dotted lines are Minkowski embeddings. Since we are interested in the case  $\tilde{m} = 0$ , the condensate is the intersect of the curves with the vertical axis. As temperature goes up the condensate moves from the lower dot to the middle curve continuously, then jumps at  $\tilde{w}_H = 0.3435$  to the origin (zero condensate), which corresponds to the chiral symmetric phase. It is also the transition from a Minkowski (dotted line) to a black hole embedding (solid line). This jump can be seen by a Maxwell construction:  $\tilde{m}$  and  $\tilde{c}$  are conjugate variables and the two areas between the middle curve and the axis are equal at the transition point. See [6] for more details.

This transition as well as restoring chiral symmetry also corresponds to the melting of bound states of the defect quarks since the Minkowski embedding has stable linearized mesonic fluctuation whilst the black hole embedding has a quasi-normal mode spectrum [18].

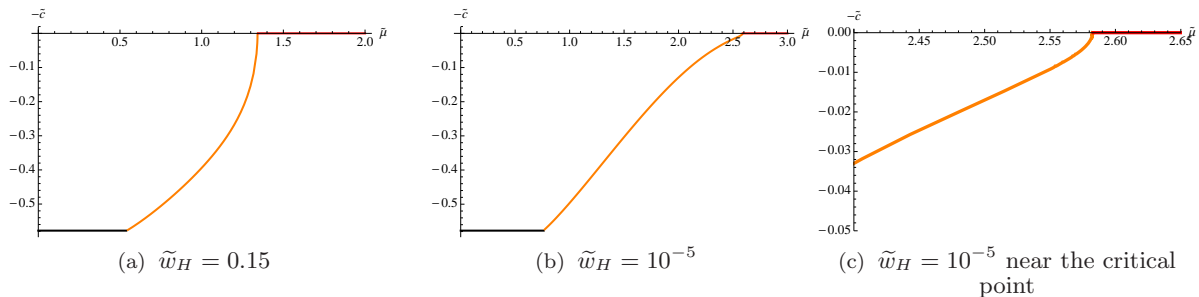


FIG. 3: Plots of the condensate vs chemical potential on fixed temperature slices, showing the phase structure of the theory. Figure (b) and (c) show that at low temperature the BKT transition becomes second order.

#### IV. CHIRAL SYMMETRY RESTORATION BY DENSITY

At zero temperature we find two phase transitions with increasing chemical potential.

At low chemical potentials the preferred embedding is a Minkowski embedding with  $\tilde{A}_t = \mu$  so there is no quark density. There is then a transition to a black hole embedding with non-zero quark density,  $\tilde{d}$ . This transition, whilst appearing first order in terms of the brane embeddings, displays second order behaviour in all field theory quantities such as the condensate or density (which grows smoothly from zero). The transition also corresponds to the on set of bound state melting since the black hole embedding has quasi-normal modes rather than stable fluctuations.

The chiral symmetry transition induced by density at zero temperature is distinct and also a continuous transition. It has been shown to be of the BKT type for this D3/D5 case [7] as opposed to a mean-field type second order transition as seen in the D3/D7 case [4, 5].

The chiral symmetric phase corresponds to the trivial embedding,  $L = 0$ . Chiral symmetry breaking is signaled by the instability of small fluctuation around the  $L = 0$  embedding. The Free energy (15) with (9) at zero T reads

$$\tilde{F} \sim \sqrt{1 + \tilde{L}'^2} \sqrt{\tilde{\rho}^4 + \frac{\rho^4}{\tilde{w}^4} + \tilde{d}^2}, \quad (17)$$

which can be expanded up to the quadratic order in  $\tilde{L}$  as

$$\tilde{F} \sim -\frac{1}{2} \sqrt{1 + \tilde{\rho}^4 + \tilde{d}^2} \tilde{L}'^2 + \frac{\tilde{L}^2}{\tilde{\rho}^2 \sqrt{1 + \tilde{\rho}^4 + \tilde{d}^2}} \quad (18)$$

At  $\tilde{\rho} \gg 1$ ,  $\frac{\tilde{L}}{\tilde{\rho}}$  behaves as a scalar with  $m^2 = -2$  in  $\text{AdS}_4$ , while at small  $\tilde{\rho} \ll 1$  and  $\tilde{\rho} \ll \tilde{d}$  it behaves as a scalar with  $m^2 = -\frac{2}{1+\tilde{d}^2}$  in  $\text{AdS}_2$ . The Breitenlohner-Freedman (BF) bound of  $\text{AdS}_2$  is  $-\frac{1}{4}$ , so below  $\tilde{d}_c = \sqrt{7}$  the BF bound is violated and the embedding  $\tilde{L} = 0$  is unstable [7]. This critical density corresponds to the critical

chemical potential  $\tilde{\mu} \sim 2.9$  as can be computed from (14). In [7] it was shown that the condensate scales near this transition as

$$-\tilde{c} \sim -e^{-\pi \sqrt{\frac{1+\tilde{d}^2}{\tilde{d}^2 - \tilde{d}^2}}}, \quad (19)$$

which corresponds to BKT scaling [11]. This transition is an example of the analysis in [12] where it was shown that if a scalar mass in a holographic model could be tuned through the BF bound a BKT transition would be seen at the critical point.

#### V. PHASE DIAGRAM IN $\mu$ -T PLANE

To compute the full phase diagram we work on a series of constant T slices. We have found the four relevant embeddings discussed above and found those that minimize the relevant thermodynamic potential. For more details of the method and relevant analysis we refer to [4], where we studied D3/D7 system using the same methods. Fig 3 shows some example plots of the dependence of the condensate on the density on fixed T slices. It shows that the Minkowski embedding with  $\tilde{d} = 0$  is preferred at low  $\tilde{\mu}$ , a black hole embedding with growing  $\tilde{d}$  at intermediate  $\tilde{\mu}$ , before finally a transition to a flat embedding occurs at high chemical potential.

Qualitatively the phase diagram, shown in Fig 1, is almost the same as the D3/D7 case - the two second order transitions at zero temperature converge at two critical points to form the first order transition identified at zero density. The only difference is induced by the chiral phase transition at zero T. Comparing to the D3/D7 case we see there is a long tail near zero T, the end point of which corresponds to the BKT transition. However even infinitesimal temperature turns it into mean-field type second order transition [7, 8]. In Fig 3bc we plot the condensate against  $\mu$  at a very low temperature ( $\tilde{w}_H = 10^{-5}$ ) to show the second order nature.

**Acknowledgements:** NE and KK are grateful for the support of an STFC rolling grant. KK would like to

thank Kristan Jensen and Veselin Filev for discussions. AG and MM are grateful for University of Southampton

Mayflower Scholarships.

- 
- [1] V. G. Filev, C. V. Johnson, R. C. Rashkov and K. S. Viswanathan, *JHEP* **0710**, 019 (2007) [arXiv:hep-th/0701001].
- [2] T. Albash, V. G. Filev, C. V. Johnson and A. Kundu, *JHEP* **0807**, 080 (2008) [arXiv:0709.1547 [hep-th]]
- [3] V. G. Filev, *JHEP* **0804**, 088 (2008) [arXiv:0706.3811 [hep-th]];  
J. Erdmenger, R. Meyer and J. P. Shock, *JHEP* **0712**, 091 (2007) [arXiv:0709.1551 [hep-th]];  
V. G. Filev and C. V. Johnson, *JHEP* **0810**, 058 (2008) [arXiv:0805.1950 [hep-th]];  
A. V. Zayakin, *JHEP* **0807** (2008) 116 [arXiv:0807.2917 [hep-th]];  
V. G. Filev, C. V. Johnson and J. P. Shock, *JHEP* **0908**, 013 (2009) [arXiv:0903.5345 [hep-th]];  
E. D'Hoker and P. Kraus, *JHEP* **0910**, 088 (2009) [arXiv:0908.3875 [hep-th]];  
E. D'Hoker and P. Kraus, *JHEP* **1003**, 095 (2010) [arXiv:0911.4518 [hep-th]];  
E. D'Hoker and P. Kraus, *JHEP* **1005**, 083 (2010) [arXiv:1003.1302 [hep-th]].
- [4] N. Evans, A. Gebauer, K. Y. Kim and M. Magou, arXiv:1002.1885 [hep-th].
- [5] K. Jensen, A. Karch and E. G. Thompson, arXiv:1002.2447 [hep-th].
- [6] V. G. Filev, *JHEP* **0911**, 123 (2009) [arXiv:0910.0554 [hep-th]].
- [7] K. Jensen, A. Karch, D. T. Son and E. G. Thompson, arXiv:1002.3159 [hep-th].
- [8] N. Iqbal, H. Liu, M. Mezei and Q. Si, arXiv:1003.0010 [hep-th].
- [9] A. Karch and E. Katz, *JHEP* **0206**, 043 (2002) [arXiv:hep-th/0205236];  
M. Grana and J. Polchinski, *Phys. Rev. D* **65** (2002) 126005, [arXiv: hep-th/0106014];  
M. Bertolini, P. Di Vecchia, M. Frau, A. Lerda and R. Marotta, *Nucl. Phys. B* **621**, 157 (2002) [arXiv:hep-th/0107057];  
M. Kruczenski, D. Mateos, R. C. Myers and D. J. Winters, *JHEP* **0307** 049, 2003 [arXiv:hep-th/0304032].  
J. Erdmenger, N. Evans, I. Kirsch and E. Threlfall, *Eur. Phys. J. A* **35** (2008) 81 [arXiv:0711.4467 [hep-th]].
- [10] A. Karch and L. Randall, *JHEP* **0106** (2001) 063 [arXiv:hep-th/0105132].  
O. DeWolfe, D. Z. Freedman and H. Ooguri, *Phys. Rev. D* **66** (2002) 025009 [arXiv:hep-th/0111135].  
J. Erdmenger, Z. Guralnik and I. Kirsch, *Phys. Rev. D* **66** (2002) 025020 [arXiv:hep-th/0203020];  
R. C. Myers and M. C. Wapler, *JHEP* **0812**, 115 (2008) [arXiv:0811.0480 [hep-th]];  
M. C. Wapler, *Int. J. Mod. Phys. A* **25**, 4397 (2010) [arXiv:0909.1698 [hep-th]];  
M. C. Wapler, *JHEP* **1001**, 056 (2010) [arXiv:0911.2943 [hep-th]];  
M. C. Wapler, *JHEP* **1005**, 019 (2010) [arXiv:1002.0336 [hep-th]].
- [11] V. L. Berezinskii, *Zh. Eksp. Theo. Fiz* **59**, 907 (1970);  
J. M. Kosterlitz and D. J. Thouless, *J. Phys. C C* **6** (1973) 1181.
- [12] D. B. Kaplan, J. W. Lee, D. T. Son and M. A. Stephanov, "Conformality Lost," *Phys. Rev. D* **80**, 125005 (2009) [arXiv:0905.4752 [hep-th]].
- [13] J. M. Maldacena, *Adv. Theor. Math. Phys.* **2**, 231 (1998) *Int. J. Theor. Phys.* **38**, 1113 (1999) [arXiv:hep-th/9711200];  
E. Witten, *Adv. Theor. Math. Phys.* **2** (1998) 253 [arXiv:hep-th/9802150];  
S. S. Gubser, I. R. Klebanov and A. M. Polyakov, *Phys. Lett. B* **428** (1998) 105 [arXiv:hep-th/9802109].
- [14] S. Kobayashi, D. Mateos, S. Matsuura, R. C. Myers and R. M. Thomson, *JHEP* **0702**, 016 (2007) [arXiv:hep-th/0611099];
- [15] K. Y. Kim, S. J. Sin and I. Zahed, arXiv:hep-th/0608046;  
K. Y. Kim, S. J. Sin and I. Zahed, *JHEP* **0801**, 002 (2008) [arXiv:0708.1469 [hep-th]];  
K. Y. Kim and J. Liao, *Nucl. Phys. B* **822**, 201 (2009) [arXiv:0906.2978 [hep-th]].
- [16] D. Mateos, S. Matsuura, R. C. Myers and R. M. Thomson, *JHEP* **0711** (2007) 085 [arXiv:0709.1225 [hep-th]].
- [17] J. Babington, J. Erdmenger, N. J. Evans, Z. Guralnik and I. Kirsch, *Phys. Rev. D* **69** (2004) 066007 [arXiv:hep-th/0306018];  
R. Apreda, J. Erdmenger, N. Evans and Z. Guralnik, *Phys. Rev. D* **71** (2005) 126002 [arXiv:hep-th/0504151];  
T. Albash, V. G. Filev, C. V. Johnson and A. Kundu, *Phys. Rev. D* **77** (2008) 066004 [arXiv:hep-th/0605088];  
D. Mateos, R. C. Myers and R. M. Thomson, *Phys. Rev. Lett.* **97** (2006) 091601 [arXiv:hep-th/0605046];  
D. Mateos, R. C. Myers and R. M. Thomson, *JHEP* **0705**, 067 (2007) [arXiv:hep-th/0701132].
- [18] C. Hoyos-Badajoz, K. Landsteiner and S. Montero, *JHEP* **0704**, 031 (2007) [arXiv:hep-th/0612169];  
K. Peeters, J. Sonnenschein and M. Zamaklar, *Phys. Rev. D* **74** (2006) 106008 [arXiv:hep-th/0606195].  
J. Erdmenger, M. Kaminski and F. Rust, *Phys. Rev. D* **77**, 046005 (2008) [arXiv:0710.0334 [hep-th]];  
J. Erdmenger, C. Greubel, M. Kaminski, P. Kerner, K. Landsteiner and F. Pena-Benitez, arXiv:0911.3544 [hep-th].